nature photonics

ARTICLES

PUBLISHED ONLINE: 22 FEBRUARY 2009 | DOI: 10.1038/NPHOTON.2009.4

Stereometamaterials

Na Liu[1], Hui Liu[2], Shining Zhu[2] and Harald Giessen[1]*

The subdiscipline of chemistry that studies molecular structures in three dimensions is called stereochemistry. One important aspect of stereochemistry is stereoisomers: materials with the same chemical formula but different spatial arrangements of atoms within molecules. The relative positions of atoms have great influence on the properties of chemical substances. Here, in analogy to stereoisomers in chemistry, we propose a new concept in nanophotonics, namely stereometamaterials, which refer to metamaterials with the same constituents but different spatial arrangements. As a model system of stereometamaterials, we theoretically and experimentally study meta-dimers, which consist of a stack of two identical split-ring resonators in each unit cell with various twist angles. The interplay of electric and magnetic interactions plays a crucial role for the optical properties. Specifically, the influence of higher-order electric multipoles becomes clearly evident. The twisting of stereometamaterials offers a way to engineer complex plasmonic nanostructures with a tailored electromagnetic response.

The word 'stereo' in Greek means 'relating to space' or 'three-dimensional'. In stereochemistry, the characteristics of organic compounds depend not only on the nature of the atoms comprising the molecules (constitution) but also on the three-dimensional arrangement of these atoms in space (configuration)[1]. For example, the spatial structure of a protein molecule determines its biological activities. In photonics, metamaterials are structured media, consisting of artificial 'atoms' with unit cells much smaller than the wavelength of light[2–4]. Such metamaterial atoms can be designed to yield electric as well as magnetic dipole moments, leading to effective negative permittivity and negative permeability. A medium with simultaneous negative permittivity and negative permeability can exhibit negative refraction and unique reversed electromagnetic properties[5,6]. As well as their applicability in constructing effective media, metamaterials have also been used as prototypes for studying coupling effects between artificial atoms in three-dimensional structures[7–9]. However, the mechanism of interactions arising from different spatial arrangements of such atoms has thus far not been examined. Inspired by the concept of stereochemistry, we now investigate the coupling effects of artificial atoms in three-dimensional metamaterials from a novel perspective. We study a set of stereometamaterials, each having unit cells consisting of two stacked split-ring resonators (SRRs) with identical geometry (same constitution); however, the two SRR atoms are arranged in space using different twist angles to achieve various structures (different configurations). We term these structures stereo-SRR dimers. We theoretically and experimentally demonstrate that the optical properties of these stereo-SRR dimers can be substantially modified by altering the twist angles between the two SRR atoms, arising from the variation of electric and magnetic interactions between them. Specifically, we investigate how the electric and magnetic interactions depend on the spatial arrangement of these SRR constituents. The nontrivial magnetic interaction makes metamaterials more versatile in nanophotonics than stereoisomers in chemistry, where generally only electric interactions are taken into account. Furthermore, we show that the inclusion of the higher-order electric multipolar interactions is essential to understanding the physical implications of the twisting dispersion. A theoretical model based on a Langrangian formalism is used to interpret the evolution of the coupling effects as a function of twist angle.

Stereometamaterial design

Figure 1a illustrates the geometry of the stereo-SRR dimer metamaterials together with their design parameters. Each unit cell consists of two spatially separated SRRs, which are twisted at an angle φ with respect to one another. The SRRs are embedded in a homogeneous dielectric with $\varepsilon = 1$ (that is, air). For excitation of these SRR dimer metamaterials, we use normally incident light with its polarization along the x-direction as shown in Fig. 1a. In order to gain insight into the resonant behaviour as well as coupling mechanisms for various stereo-SRR dimer metamaterials, we first study three specific dimer systems with twist angles $\varphi = 0$, 90 and 180°. The insets of Fig. 1b–d present the schematics of the three structures, in which the vertical distance between two SRRs is set at $s = 100$ nm. Numerical simulations were performed based on a commercial finite-integration time-domain algorithm, and the simulated transmittance spectra are shown in Fig. 1b–d. For each system there are apparently two observable resonances (ω^- and ω^+). To understand these spectral characteristics, current and magnetic field distributions at the relevant resonances are calculated. For the 0° twisted SRR dimer metamaterial, the electric component of the incident light can excite circulating currents along the two SRRs, giving rise to induced magnetic dipole moments in the individual SRRs. As shown in Fig. 2a, the electric dipoles excited in the two SRRs oscillate anti-phase and in-phase at resonances ω_0^- and ω_0^+, respectively. The resulting magnetic dipoles are aligned antiparallel at resonance ω_0^-, whereas they are parallel at resonances ω_0^+. The above phenomenon can be interpreted as the plasmon hybridization[10–12] between the two SRRs due to their close proximity. In the hybridization scheme, each SRR can be regarded as an artificial atom. The two SRR atoms are bonded into an SRR dimer or SRR 'molecule' due to the strong interaction between them. Such interaction leads to the formation of new plasmonic modes, arising from the hybridization of the original state of an individual SRR. For the configuration of the 0° twisted SRR dimer system, the two excited electric dipoles are transversely coupled, while the two magnetic dipoles are longitudinally coupled. In the case of a transverse dipole–dipole interaction, the antisymmetric and symmetric modes are at the lower and higher resonance frequencies, respectively. In contrast, in the

[1]4. Physikalisches Institut, Universität Stuttgart, D-70569 Stuttgart, Germany, [2]Department of Physics, Nanjing University, Nanjing 210093, People's Republic of China; *e-mail: Giessen@physik.uni-stuttgart.de

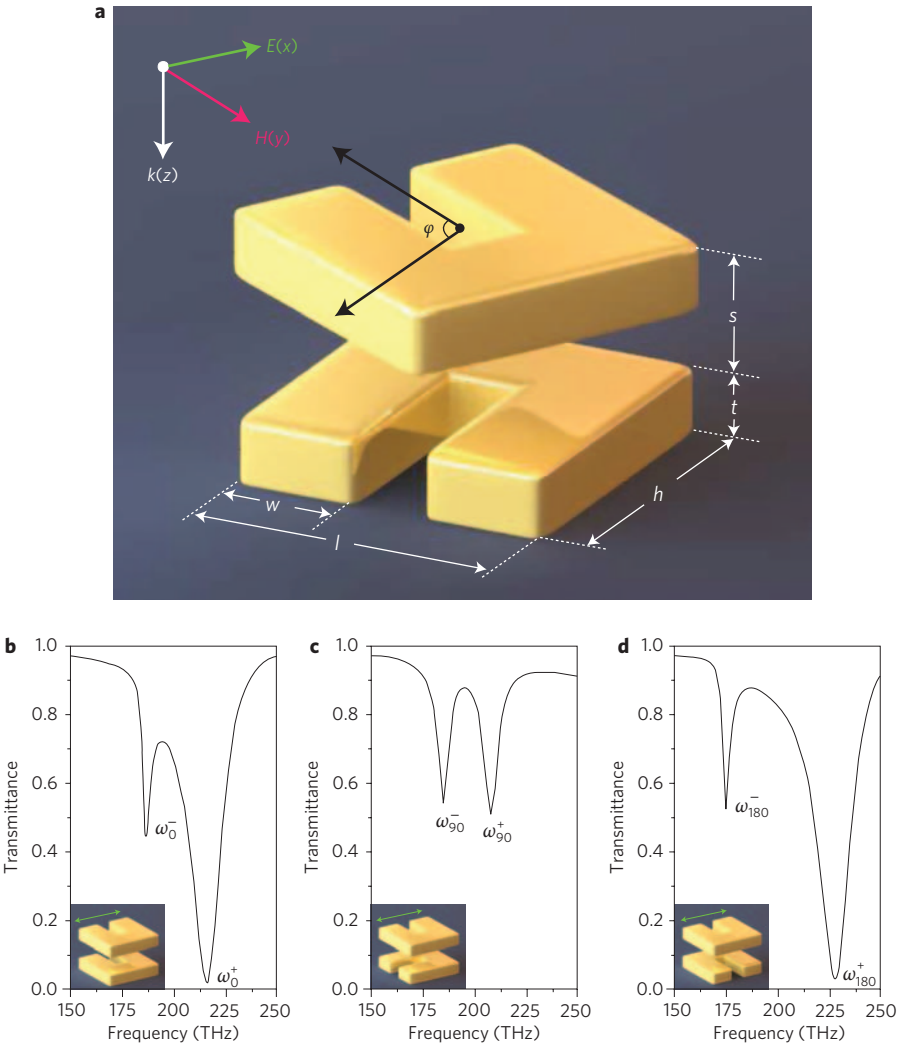

Figure 1 | Structural geometry and numerical simulation. a, Schematic of the stereo-SRR dimer metamaterials with definitions of the geometrical parameters: $l = 230$ nm, $h = 230$ nm, $w = 90$ nm, $t = 50$ nm, and $s = 100$ nm. The periods in both x and y directions are 700 nm. **b**–**d**, Simulated transmittance spectra for the 0° (**b**), 90° (**c**) and 180° (**d**) twisted SRR dimer metamaterials. All the structures are embedded in air.

case of longitudinal dipole–dipole interaction, the two magnetic dipoles should align parallel at the lower resonance frequency and antiparallel at the higher resonance frequency[12]. It is evident that for the 0° twisted SRR dimer system (see Fig. 2a), the resonance levels are determined according to the picture of transverse electric dipole–dipole interaction, with the antisymmetric (symmetric) mode having the lower (higher) resonance frequency. In essence, the two coupling mechanisms, that is, the electric and magnetic dipolar interactions, counteract one another and the electric interaction dominates in this system.

For the 90° twisted SRR dimer metamaterial, circular currents in the underlying SRR cannot be directly excited by the incident light due to its orientation with respect to the external electric field. In a sense, the underlying SRR can be regarded as a 'dark atom' at the resonant frequency of the ring[13]. Nevertheless, for the coupled dimer system, on resonance, excitation from the upper SRR can be transferred to the underlying one by the interaction between the two SRRs, which can also lead to the formation of new plasmonic modes (ω_{90}^- and ω_{90}^+). Interestingly, because the electric fields in the slit gaps of the two SRRs are perpendicular to one another, the electric dipole–dipole interaction equals zero. In addition, as the higher-order multipolar interaction is negligible in a first approximation, the electric coupling in the 90° twisted SRR dimer system can thus be ignored. As a consequence, the resonance levels are determined in line with the picture of longitudinal magnetic dipole–dipole coupling. As shown in Fig. 2b, at resonances ω_{90}^- and ω_{90}^+, the resulting magnetic dipoles in the two SRRs are aligned parallel and antiparallel, respectively.

For the 180° twisted SRR dimer metamaterial, the interaction between the two SRRs results in new plasmonic modes, ω_{180}^- and ω_{180}^+. Notably, from the current and magnetic field distributions as shown in Fig. 2c, resonances ω_{180}^- and ω_{180}^+ are associated with the excitation of the electric dipoles in the two SRRs oscillating anti-phase and in-phase, respectively. The two resulting magnetic dipoles are aligned parallel and antiparallel, accordingly. In essence, the transverse electric and longitudinal magnetic interactions contribute positively in the 180° twisted SRR dimer system. This leads to the largest spectral splitting, which is a direct indication of the coupling strength. Based on the above discussions, we infer that the optical properties of stereometamaterials depend dramatically on the spatial arrangement of metamaterial constituents. Specifically, the possibility of tuning the resonant behaviour by simply varying the relative twist angles makes stereometamaterials particularly interesting as model systems for exploring and comprehending different coupling mechanisms in complex three-dimensional plasmonic structures.

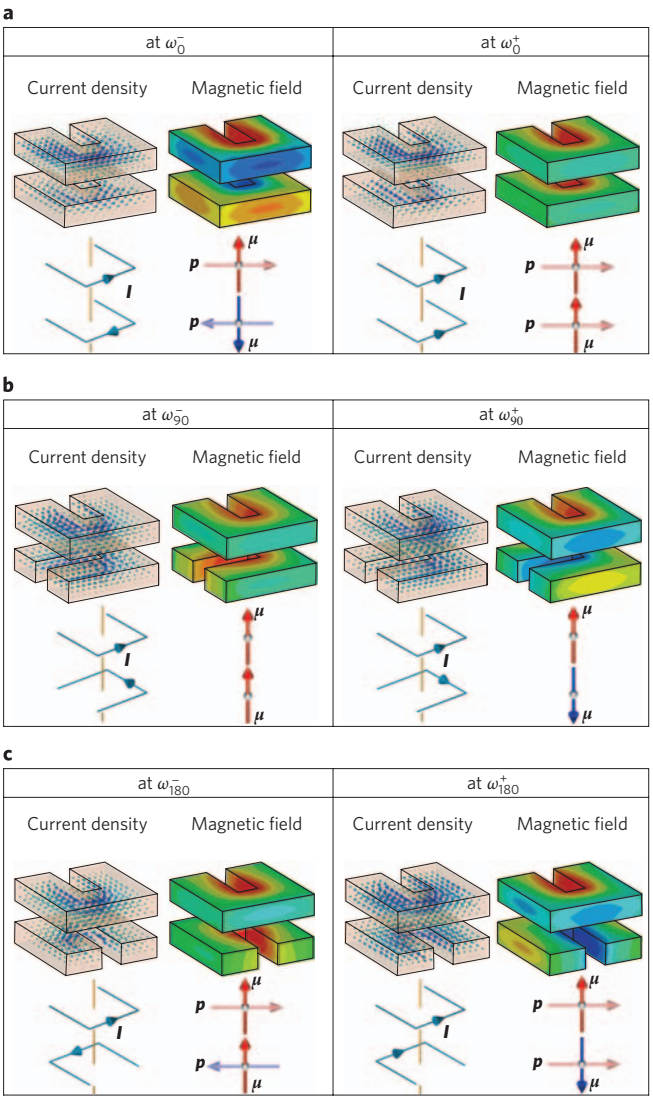

Figure 2 | Numerical current and magnetic field distributions. a–c, Current and magnetic field distributions at respective resonances for the 0° (**a**), 90° (**b**) and 180° (**c**) twisted SRR dimer metamaterials. Lower left: schematics of currents (***I***) in two SRRs. Lower right: schematics of the alignments of the magnetic (μ) and electric (p) dipoles. At 0°, transverse electric and longitudinal magnetic interactions work against one another, whereas at 180° they add together. At 90°, only longitudinal magnetic interaction is present.

Twist angle

To provide deeper insight, the dependence of the optical properties of the stereo-SRR dimer metamaterials on twist angle is investigated. Figure 3 presents the simulated twisting dispersion curves (black squares) of these stereometamaterials, in which the resonance positions are extracted from the transmittance spectra of different structures. It is apparent that by increasing the twist angle φ, the two resonance branches first tend to converge, with the ω^+ branch shifting to lower frequencies, while the ω^- branch shifts to higher frequencies. An avoided crossing is observed at φ_t, which is around 60°. Subsequently, the two branches shift away from one another. In order to clarify the underlying physics of the twisting dispersion curves, we introduce a Lagrangian formalism[14]. We start from the analysis of a single SRR and then expand it to coupled stereo-SRR dimer systems. One SRR can be modelled by an equivalent LC circuit with a resonance frequency $\omega_f = 1/(LC)^{1/2}$. It consists of a magnetic coil (the metal ring)

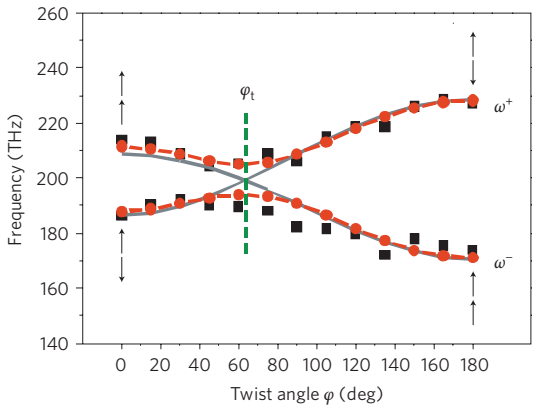

Figure 3 | Twisting dispersion of the stereo-SRR dimer metamaterials. Black squares represent the numerical data. Red lines represent the fitting curves calculated from the Lagrangian model, in which the avoided crossing is clearly visible at φ_t. The black arrows represent the alignment of the magnetic dipoles at lower and higher resonance frequencies at twist angles $\varphi = 0°$ and 180°. The grey lines represent the fitting curves calculated from the Lagrangian model without considering the higher-order electric multipolar interactions. No avoided crossing is observable in this case.

with inductance L and a capacitor (the slit of the ring) of capacitance C. If we define the total charge Q accumulated in the slit as a generalized coordinate, the Lagrangian of an SRR can be written as $\Gamma = (L\dot{Q}^2/2) - (Q^2/2C)$. Here, $L\dot{Q}/2$ refers to the kinetic energy of the oscillations, and $Q^2/2C$ is the electrostatic energy stored in the slit. Consequently, the Lagrangian of the coupled SRR dimer systems is a combination of two individual SRRs with the additional electric and magnetic interaction terms

$$\Gamma = \frac{L}{2}\left(\dot{Q}_1^2 - \omega_f^2 Q_1^2\right) + \frac{L}{2}\left(\dot{Q}_2^2 - \omega_f^2 Q_2^2\right) + M_H \dot{Q}_1 \dot{Q}_2 - M_E \omega_f^2 Q_1 Q_2 \cdot \left(\cos\varphi - \alpha \cdot (\cos\varphi)^2 + \beta \cdot (\cos\varphi)^3\right) \quad (1)$$

Here, Q_1 and Q_2 are oscillating charges in the respective SRRs, and M_H and M_E are the mutual inductances for the magnetic and electric interactions, respectively. Apart from the electric dipole–dipole interaction, the contributions from the higher-order electric multipolar[15] interactions are also included. α and β are the coefficients of the quadrupolar and octupolar plasmon interactions[16], respectively. They serve as correction terms to the electric dipolar interaction. It is straightforward to derive from equation (1) that the major interaction items for 0° and 180° cases are $M_H\dot{Q}_1\dot{Q}_2 - M_E\omega_f^2 Q_1 Q_2$ and $M_H\dot{Q}_1\dot{Q}_2 + M_E\omega_f^2 Q_1 Q_2$, respectively. It is in accord with the above simulation results that the magnetic and electric interactions contribute oppositely and positively for 0° and 180° twisted SRR dimer metamaterials, respectively. For the 90° twisted SRR dimer metamaterial, only the magnetic interaction plays a key role, as represented by the interaction term $M_H\dot{Q}_1\dot{Q}_2$. Subsequently, by solving the Euler–Lagrange equations

$$\frac{d}{dt}\left(\frac{\partial\Gamma}{\partial\dot{Q}_i}\right) - \frac{\partial\Gamma}{\partial Q_i} = 0, \quad i = 1, 2 \quad (2)$$

the eigenfrequencies of these stereo-SRR dimer systems can be obtained as

$$\omega_\pm = \omega_0 \cdot \sqrt{\frac{1 \mp \kappa_E \cdot \left(\cos\varphi - \alpha \cdot (\cos\varphi)^2 + \beta \cdot (\cos\varphi)^3\right)}{1 \mp \kappa_H}} \quad (3)$$

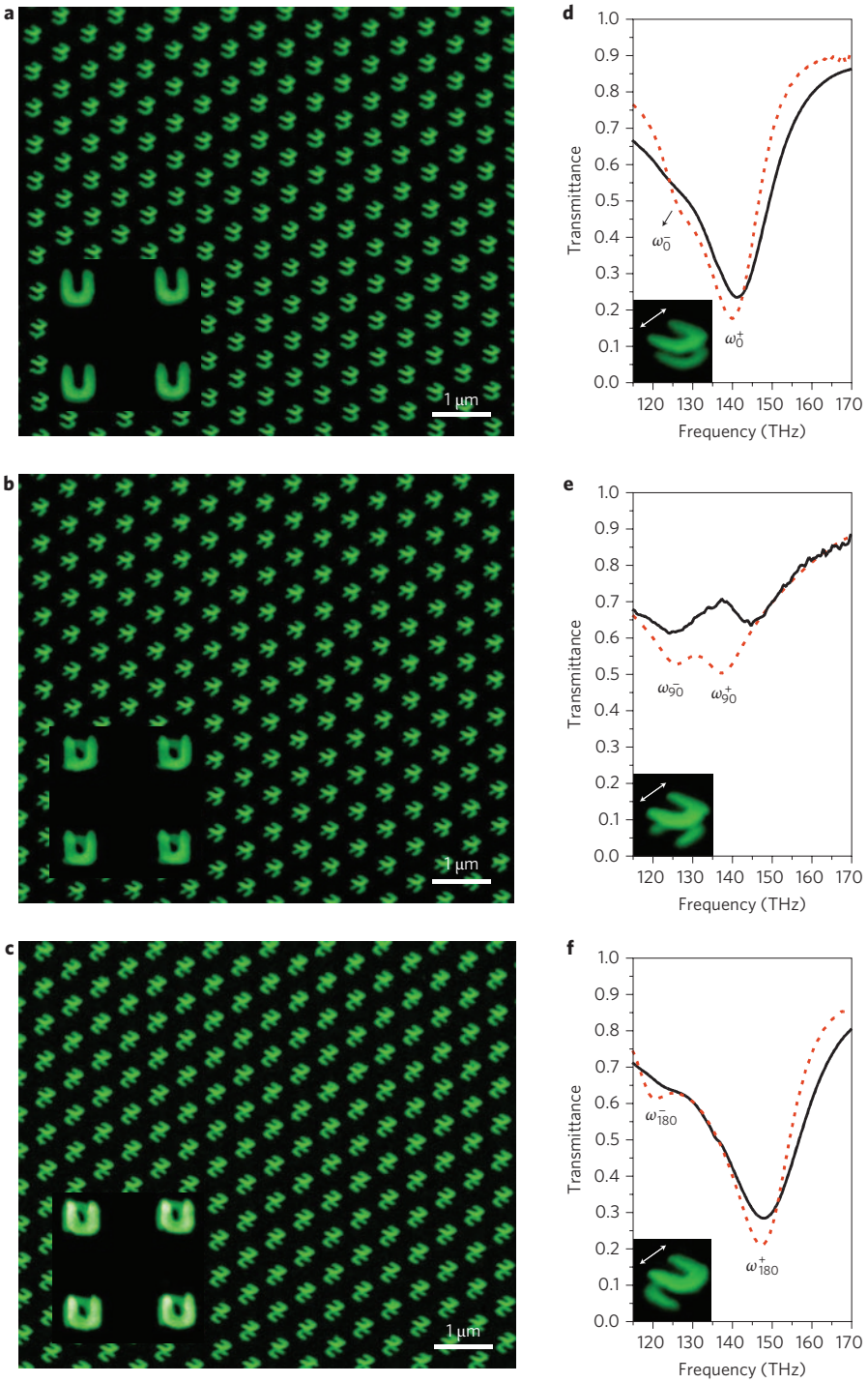

Figure 4 | Field-emission electron microscopy images and experimental measurement. a–c, Oblique views of the 0° (**a**), 90° (**b**) and 180° (**c**) twisted gold SRR dimer metamaterials. Insets: normal views. The structures were fabricated on a glass substrate. The SRRs were embedded in a photopolymer (PC403), which served as the dielectric spacer. **d–f**, Experimental transmittance spectra for the 0° (**d**), 90° (**e**), and 180° (**f**) twisted SRR dimer metamaterials. The black and red curves represent the experimental and simulated results, respectively. For the 90° twisted SRR dimer structure, an analyser is applied behind the sample, which is rotated by 75° with respect to the polarization of the incident light.

where $\kappa_E = M_E/L$ and $\kappa_H = M_H/L$ are the coefficients of the overall electric and magnetic interactions, respectively. By fitting the twisting dispersion curves, the corresponding coefficients are estimated to be $\kappa_E = 0.14$, $\kappa_H = 0.09$, $\alpha = 0.8$ and $\beta = -0.4$. Notably from Fig. 3, the fitting curves (in red lines) reproduce the numerical data quite well and the avoided crossing is clearly observable around 60°. This shows that the Lagrangian model can quantitatively corroborate the results from the numerical simulations. It is of crucial importance that the higher-order electric multipolar interactions account for the existence of the avoided crossing. Owing to the finite length of the SRR ring, discrete electric plasmon modes characterized by different spatial symmetries can be excited by the incident light. The surface charges in the SRR ring are a superposition of such fundamental plasmon modes of the ring[16].

To reveal the significant role of the higher-order electric multipolar interactions, the grey lines in Fig. 3 display the twisting dispersion curves, in which only the dipolar coupling effect is taken into account; that is, $\alpha = 0$ and $\beta = 0$. The best fit is achieved with $\kappa_E = 0.2$ and $\kappa_H = 0.09$. Obviously, despite the fact that the grey curves can fit most parts of the numerical data, no avoided crossing is predicted. Instead, the ω^+ and ω^- branches converge at φ_t. Therefore, it has to be emphasized that although the electric and magnetic dipolar interactions are the essential mechanisms, the higher-order electric multipolar interactions should also be carefully considered for fully understanding the origin of the spectral characteristics of the stereometamaterial systems.

The angle where the avoided crossing occurs in the twisting dispersion spectrum is correlated with the geometry of the SRRs as well as the vertical distance between the two SRRs. For the specific stereo-SRR dimer metamaterials we investigated here, the avoided crossing appears at ~60°. Based on detailed simulated field distribution studies, we found that this angle is also a transition angle where the higher and lower frequency modes exchange their magnetic dipole alignments from parallel to antiparallel. At angles smaller than angle φ_t, the two magnetic dipoles are aligned parallel (antiparallel) at resonance ω^+ (ω^-). The electric coupling effect dominates in this regime. With continuous increase of the twist angle, due to the displacement of the two SRRs, the electric coupling contributes less effectively. Consequently, the splitting of the two resonance branches starts to decrease. This situation remains until the transition angle is reached, where the electric and magnetic dipole–dipole interactions cancel one another. The higher-order electric multipolar interactions account for the avoided crossing of the two resonance branches. After angle φ_t, the electric coupling continues to decrease. As a result, the resonance levels are determined according to the scheme of magnetic dipole–dipole coupling, that is, the parallel and antiparallel alignments of the magnetic dipoles in the two SRRs correspond to the lower and higher frequency resonances, respectively. When the twist angle reaches 90°, the electric coupling quenches and is negligible. This represents a purely magnetic dipole–dipole coupling situation. Subsequently, with further increase of the twist angle, the displacement of the two SRRs is reduced and the electric coupling comes into play again. Because of the orientation of the two SRRs, the electric and magnetic coupling can contribute positively, giving rise to a larger splitting of the two resonance branches with increasing twist angle. The splitting finally reaches its maximum at $\varphi = 180°$.

The structures of stereometamaterials are compatible with nanofabrication stacking techniques[7,9]. We fabricated three stereo-SRR dimer metamaterials with specific twist angles $\varphi = 0$, 90 and 180°, as illustrated in the insets of Fig. 1b–d. In the experiment, the structures were fabricated on a glass substrate. Gold SRRs were embedded in a photopolymer (PC403), which served as the dielectric spacer. A spacer of $s = 120$ nm was applied in order to achieve surface planarization for stacking the second SRR layer. The electron micrographs of the fabricated SRR dimer metamaterials were obtained by field-emission scanning electron microscopy. Figure 4a–c presents oblique views of the 0, 90 and 180° twisted SRR dimer metamaterials, in which the underlying SRRs are clearly visible. The insets of Fig. 4a–c show the normal views, demonstrating the good accuracy of lateral alignment for the different SRR layers. To experimentally investigate the optical properties of these SRR dimer metamaterials, the near-infrared transmittance spectra of the samples at normal incidence were measured by a Fourier-transform infrared spectrometer with electric field polarization as illustrated in Fig. 1. The measured transmittance spectra are presented by black curves in Fig. 4d–f and the simulated spectra as red dashed curves. The resonance positions are redshifted compared to those of the corresponding resonances in Fig. 1b–d due to the presence of glass substrate and dielectric spacers. For a reasonable comparison with the experiment, in the simulations in Fig. 4d–f, gold with a three times higher damping constant as that used in Fig. 1b–d was used to account for the surface scattering and grain boundary effects in the thin film of the real systems[17]. The overall qualitative agreement between experimental and simulated results is quite good. The discrepancies are most likely due to tolerances in fabrication and assembly, as well as significant broadening in the experiment. For 0° and 180° twisted SRR dimer structures, the lower resonances ω_0^- and ω_{180}^- are less distinctly visible than the higher resonances ω_0^+ and ω_{180}^+, respectively (see spectra in Fig. 4d,f). This is due to the fact that for both dimer structures, the electric coupling plays a key role. At the lower resonance frequencies (ω_0^- and ω_{180}^-), the electric dipoles in the two SRRs oscillate anti-phase. Such resonances are not easily excited by light. On the other hand, at the higher resonance frequencies (ω_0^+ and ω_{180}^+), the electric dipoles in the two SRRs oscillate in-phase. Such resonances can strongly couple to light. For the 90° twisted SRR dimer structure, the splitting of the resonances is clearly observable when an analyser is applied behind the sample, which is rotated by 75° with respect to the polarization of the incident light. This is due to the polarization rotation effect arising from the chirality[18,19] of the 90° twisted structure.

The new concept of stereometamaterials adds a significant degree of freedom through the interplay of electric and magnetic interactions, and tremendously enhances the versatility of nanophotonic structures. Stereometamaterials allow us to use higher-order electric multipolar as well as magnetic interactions, which can be nearly as large as the electric dipolar interaction. This is completely different from molecules, where electric dipolar interaction is the essential contribution determining optical properties. It will also be interesting to study the geometry and distance dependence of the different coupling effects. Our concept can be extended to more complex artificial molecules, such as stereotrimers, stereoquadrumers and so on. The tuneability of the resonant behaviour of these new artificial materials by altering the spatial arrangement of their constituents offers great flexibility for exploring useful metamaterial applications, such as chiral structures with negative refraction[20], invisibility cloaks[21] and magneto-optically active materials[22]. Stereometamaterials open up the potential for optical polarization control, which so far has been dominated by stereoisomers[1] and liquid crystals[23]. (See Supplementary Information for more details on optical stereoisomers as well as left- and right-handed enantiomers.) Stereometamaterials might also serve as artificial nanosystems for emulating the optical properties of complex biomolecules, such as double helix DNA chiral proteins and drug enzymes, which have profound application potentials in biophotonics, pharmacology, as well as diagnostics.

Methods

Structure fabrication. Three (or more) gold alignment marks (size 4 × 100 μm) with a gold thickness of 250 nm were first fabricated using a lift-off process on a quartz substrate. The substrate was then covered with a 50-nm gold film using electron-beam evaporation. Next, SRR structures were defined in negative resist (AR-N, ALLRESIST GmbH) by electron-beam lithography. Ion beam etching (Ar^+ ions) of the gold layer was then performed to generate the gold SRR structures. Subsequently, a 120-nm-thick spacer layer was applied on the first layer by spin-coating. A solidifiable photopolymer, PC403 (JCR), was used as the planarized spacer layer. A pre-baking process in which the baking temperature was continuously increased from 90 to 130 °C was first performed to remove the solvent from the polymer. A sufficiently long bake at a higher temperature (30 min in a 180 °C oven) further hardened the layer. A 50-nm gold film and a spin-coated AR-N resist layer were subsequently deposited on the sample. Next, the stacking alignment using the gold alignment marks was applied to ensure accurate stacking of the second SRR layer. The procedures of in-plane fabrication were repeated with the final layer being PC403. All structures had a total area of 200 × 200 μm.

Optical and structure characterization. Transmittance spectra were measured with a Fourier-transform infrared spectrometer (Bruker IFS 66v/S, tungsten lamp) combined with an infrared microscope (×15 Cassegrain objective, NA = 0.4, liquid

N_2-cooled MCT 77 K detector, infrared polarizer). The measured spectra were normalized with respect to a bare glass substrate.

The simulated transmittance spectra and field distributions were performed using the software package CST Microwave Studio. For the spectra in Fig. 1b–d, the permittivity of bulk gold in the infrared spectral regime was described by the Drude model with plasma frequency $\omega_{pl} = 1.37 \times 10^{16}\ s^{-1}$ and the damping constant $\omega_c = 4.08 \times 10^{13}\ s^{-1}$. For the spectra in Fig. 4d–f, owing to the surface scattering and grain boundary effects in the thin film of the real systems, the simulation results were obtained using a damping constant that was three times larger than the bulk value. The optical parameters were the refractive index of PC403 $n_{PC403} = 1.55$ and the quartz substrate refractive index $n_{glass} = 1.5$.

The electron micrographs of the fabricated structures were taken with an FEI-Nova Nanolab 600 scanning electron microscope.

Received 13 October 2008; accepted 21 January 2009; published online 22 February 2009

References

1. Robinson, M. J. T. *Organic Stereochemistry* (Oxford Univ. Press, 2000).
2. Smith, D. R., Pendry, J. B. & Wiltshire, M. C. K. Metamaterials and negative refractive index. *Science* **305,** 788–792 (2004).
3. Soukoulis, C. M., Linden, S. & Wegener, M. Negative refractive index at optical wavelengths. *Science* **315,** 47–49 (2007).
4. Shalaev, V. M. Optical negative-index metamaterials. *Nature Photon.* **1,** 41–48 (2007).
5. Veselago, V. G. The electrodynamics of substances with simultaneously negative values of ε and μ. *Sov. Phys. Usp.* **10,** 509–514 (1968).
6. Pendry, J. B. Negative refraction makes a perfect lens. *Phys. Rev. Lett.* **85,** 3966–3969 (2000).
7. Liu, N. *et al.* Three-dimensional photonic metamaterials at optical frequencies. *Nature Mater.* **7,** 31–37 (2008).
8. Liu, N. *et al.* Plasmon hybridization in stacked cut-wire metamaterials. *Adv. Mater.* **19,** 3628–3632 (2007).
9. Liu, N., Fu, L. W., Kaiser, S., Schweizer, H. & Giessen, H. Plasmonic building blocks for magnetic molecules in three-dimensional optical metamaterials. *Adv. Mater.* **20,** 3859–3865 (2008).
10. Prodan, E., Radloff, C., Halas, N. J. & Nordlander, P. A hybridization model for the plasmon response of complex nanostructures. *Science* **302,** 419–422 (2003).
11. Wang, H., Brandl, D. W., Le, F., Nordlander, P. & Halas, N. J. Nanorice: a hybrid plasmonic nanostructure. *Nano Lett.* **6,** 827–832 (2006).
12. Nordlander, P., Oubre, C., Prodan, E., Li, K. & Stockman, M. I. Plasmon hybridization in nanoparticle dimers. *Nano Lett.* **4,** 899–903 (2004).
13. Liu, N., Kaiser, S. & Giessen, H. Magnetoinductive and electroinductive coupling in plasmonic metamaterial molecules. *Adv. Mater.* **20,** 4521–4525 (2008).
14. Liu, H. *et al.* Magnetic plasmon hybridization and optical activity at optical frequencies in metallic nanostructures. *Phys. Rev. B* **76,** 073101 (2007).
15. Rockstuhl, C. *et al.* On the reinterpretation of resonances in split-ring-resonators at normal incidence. *Opt. Express* **14,** 8827–8836 (2006).
16. Hao, F. *et al.* Shedding light on dark plasmons in gold nanorings. *Chem. Rev. Lett.* **458,** 262–266 (2008).
17. Zhang, S. *et al.* Demonstration of metal–dielectric negative-index metamaterials with improved performance at optical frequencies. *J. Opt. Soc. Am. B* **23,** 434–438 (2006).
18. Rogacheva, A. V., Fedotov, V. A., Schwanecke, A. S. & Zheludev, N. I. Giant gyrotropy due to electromagnetic-field coupling in a bilayered chiral structure. *Phys. Rev. Lett.* **97,** 177401 (2006).
19. Decker, M., Klein, M. W., Wegener, M. & Linden, S. Circular dichroism of planar chiral magnetic metamaterials. *Opt. Lett.* **32,** 856–858 (2007).
20. Pendry, J. B. A chiral route to negative refraction. *Science* **306,** 1353–1355 (2004).
21. Schurig, D. *et al.* Metamaterial electromagnetic cloak at microwave frequencies. *Science* **314,** 977–980 (2006).
22. Svirko, Y. P. & Zheludev, N. I. *Polarization of Light in Nonlinear Optics* (Wiley, 1998).
23. Scharf, T. *Polarized Light in Liquid Crystals and Polymers* (Wiley, 2007).

Acknowledgements

The authors would like to thank M. Stockman, T. Pfau, F. Giesselmann and M. Dressel for useful discussions and comments. We thank S. Linden for stimulating us to study the twisted SRRs with different angles. We acknowledge S. Hein for his metamaterial visualizations. We gratefully thank M. Hirscher and U. Eigenthaler at the Max-Planck-Institut für Metallforschung for their electron microscopy support. We acknowledge S. Kaiser, H. Graebeldinger and M. Ubl for technical assistance. This work was financially supported by Deutsche Forschungsgemeinschaft (SPP1113 and FOR557), Landesstiftung BW and BMBF (13N9155 and 13N10146). The research of H.L. and S.Z. was financially supported by the National Natural Science Foundation of China (no. 10604029, no. 10704036 and no. 10874081) and the National Key Projects for Basic Researches of China (no. 2009CB930501, no. 2006CB921804 and no. 2004CB619003).

Additional information

Supplementary Information accompanies this paper at www.nature.com/naturephotonics. Reprints and permission information is available online at http://npg.nature.com/reprintsandpermissions/. Correspondence and requests for materials should be addressed to H.G.